THE JOURNAL OF PHYSICAL CHEMISTRY C

pubs.acs.org/JPCC Article

Molecular Mechanism of Linear Polyphosphate Adsorption on Iron and Aluminum Oxides

Biao Wan, Evert J. Elzinga, Rixiang Huang,* and Yuanzhi Tang*

Cite This: https://dx.doi.org/10.1021/acs.jpcc.0c06127 Read Online

ABSTRACT: Polyphosphate is a polymeric P species with environmental and industrial significance. Understanding their interaction with natural minerals is fundamental for predicting their transport and fate in the environment. This study investigates the molecular mechanism of interaction between linear polyphosphates with varied chain length (15P, 60P, and 130P) and Fe/Al oxides using quartz crystal microbalance with dissipation (QCM-D), ^{31}P solid-state nuclear magnetic resonance (NMR) spectroscopy, and attenuated total reflection−Fourier transformed infrared (ATR−FTIR) spectroscopy. QCM-D results show that all three polyphosphates irreversibly adsorb on Fe/Al oxides at pH 4−10 with similar mass-based adsorption amounts despite the large difference in chain lengths. ATR−FTIR and NMR spectroscopy results suggest that terminal phosphate groups of the polyphosphate molecules may form bidentate binuclear surface complexes, and a fraction of middle phosphate groups may form monodentate mononuclear surface complexes on Fe/Al oxides. The interaction modes persist for both minerals and all tested pH conditions. A combination of these complementary techniques helps gain a mechanistic understanding of polyphosphate interaction with Fe/Al oxides, and the results fill a knowledge gap on polyphosphate cycling in natural environments.

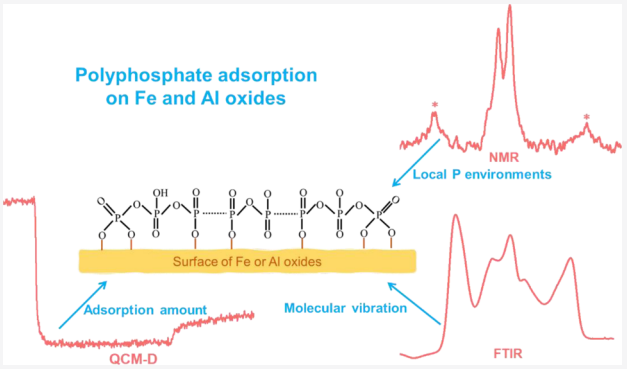

INTRODUCTION

Phosphorus (P) is an essential macro-nutrient for all living organisms.[1] In nature, P exists in a range of molecular forms, including orthophosphates, organic phosphate esters, condensed phosphates, phosphite, and phosphonates.[1,2] Polyphosphates are polymers of at least three phosphate ions joined by high-energy phosphoanhydride (P−O−P) bonds.[3,4] They can be synthesized by almost all organisms (e.g., bacteria and planktons) in terrestrial and aquatic environments and serve many important biological functions.[5−8] Polyphosphate constitutes a significant portion (1−13%) of total P in the dissolved phase, sinking particulates, and sediments, making it a key player in marine P sequestration and global P cycling.[8−10] Additionally, polyphosphate is an important industrial chemical that is widely used for mineral processing (as a dispersant), water treatment (for corrosion and scale prevention), food industry, and fertilization.[4,11] In wastewater treatment systems, polyphosphate can account for approximately 15−75% of total P in raw sewage and 5−40% of total P in secondary effluents.[12,13] The widespread use of polyphosphate will ultimately result in its release into natural environments and may cause eutrophication problems. Considering the environmental and industrial significance of polyphosphate, it is thus important to understand the biogeochemical processes (e.g., adsorption on natural minerals) governing the cycling of polyphosphate in natural environments such as soils and sediments.[10,14]

Although extensive efforts have been devoted to understanding the cycling of different P species such as orthophosphate and organic phosphates,[15,16] relatively less is known on the geochemical behaviors of polyphosphate.[17] Adsorption and desorption at the mineral−water interface play critical roles in regulating the phase distribution of various P species and their susceptibility to abiotic and biotic transformations; thus, the adsorption behavior of polyphosphate warrants detailed investigations.[18,19] Soluble polyphosphates in water columns are subject to rapid enzymatic hydrolysis into orthophosphate,[20] and surface adsorption of polyphosphate on natural minerals might affect polyphosphate enzymatic hydrolysis at the sediments−water interface. For example, a previous study proposed that adsorption on mineral surfaces might protect organic phosphates from fast enzymatic transformation by reducing the likelihood of direct hydrolysis

Received: July 4, 2020
Revised: November 8, 2020

https://dx.doi.org/10.1021/acs.jpcc.0c06127
J. Phys. Chem. C XXXX, XXX, XXX−XXX

of organic phosphates by enzymes.[21] Previous investigations on orthophosphate and organic phosphates indicated that iron (Fe) and aluminum (Al) (oxyhydr)oxides are the main mineral phases responsible for P adsorption in soils and sediments due to the strong positive charge and high surface area of these minerals at environmental pH range.[16,22−27] Adsorption of orthophosphate and organic phosphates on these minerals is generally through the formation of inner-sphere surface complexes with the phosphate moiety and is controlled by the mineral type/crystallinity, pH, and solution composition.[16,25,26,28]

A few studies have characterized the interactions between short-chained polyphosphates (2−10 phosphate units in the molecules) and Fe, Al, titanium (Ti), and zinc (Zn) oxide minerals.[13,17,29−31] The results suggest that short-chained polyphosphates can form inner-sphere surface complexes on stable Ti, Fe, and Al oxides[13,17,30,31] as well as metal phosphate precipitates on Zn oxide surface that is susceptible to dissolution and transformation.[29] For example, by applying electron delocalization and polarization to explain infrared (IR) peak shifts of triphosphate (3P) complexes on Al hydroxide, Guan et al. (2005) demonstrated that 3P can form monodentate and binuclear complexes on Al hydroxide surface.[13] In addition, a long-term (up to 3 months) investigation of 3P adsorption on goethite (α-FeOOH) in the presence of Ca found that drying resulted in the formation of a Ca−trimetaphosphate-type surface complex.[30] Despite research progress from these early efforts (such as those related to 3P complexation on mineral surfaces), detailed reaction mechanisms between long-chained polyphosphate and environmental minerals are still lacking, especially with respect to the effects of polyphosphate structures. Much also still remains unknown on the geochemical behaviors (e.g., adsorption, desorption, precipitation, and hydrolysis) of long-chained polyphosphates on environmental oxide minerals.

The objective of this study is to investigate the adsorption kinetics and mechanism of linear polyphosphates with varied chain lengths (15 to 130P) on Fe and Al oxides over a wide pH range. The selection of 15P, 60P, and 130P in this study is mainly based on the consideration of the environmental relevance of long-chained polyphosphates. Adsorption is studied primarily using quartz crystal microbalance with dissipation (QCM-D). QCM-D possesses unique features for studying interfacial reactions as (1) it monitors adsorption mass almost in real-time and thus can quantify high-resolution adsorption kinetics and (2) it provides energy dissipation information that can be used to compare the configuration of sorbate on different mineral surfaces. Molecular interactions are characterized by complementary techniques, including solution and solid-state ^{31}P nuclear magnetic resonance (NMR) and in situ attenuated total reflectance−Fourier transform infrared (ATR−FTIR) spectroscopy.

MATERIALS AND METHODS

Materials. Polyphosphates (sodium salt) with average chain lengths of 15, 60, and 130 phosphate units were generously provided by Dr. Toshikazu Shiba (RegeneTiss Inc., Tokyo, Japan) and are hereinafter referred to as 15P, 60P, and 130P, respectively. These polyphosphates were size fractionated and purified by gel electrophoresis and characterized by gel permeation chromatography.[20] The molecular weight of these polyphosphates was calculated based on an ideal molecular formula: $P_nO_{3n+1}Na_{n+2}$, where n is the number of P atoms in the molecule or P chain length. High-purity gamma-alumina (γ-Al_2O_3) and hematite (α-Fe_2O_3) were purchased from Sky Spring Nanomaterials Inc. and Sigma-Aldrich, respectively, and were used as-is without further treatment. γ-Al_2O_3 is an analogue to naturally occurring Al (oxy)hydroxides and Al-rich clay minerals and has been widely used to represent Al oxides in numerous studies on the sorption of nutrients and metals.[17,32] α-Fe_2O_3 is a representative and common Fe (oxyhydr)oxide in nature.[16,33] Therefore, γ-Al_2O_3 and α-Fe_2O_3 were selected as adsorbent substrates to study polyphosphate adsorption on environmental oxide minerals. Both materials have been extensively characterized for their purity, mineralogy, surface area, particle size, and morphological features.[22,34]

In Situ Adsorption Measurement by QCM-D. Adsorption of polyphosphates to model Fe and Al oxide surfaces was investigated using QCM-D (Q-Sense E4, Biolin Scientific, Sweden), which consists of four flow-through modules. The working principle and data interpretation of QCM-D have been reviewed.[35,36] Briefly, QCM monitors the changes in the resonance frequency (Δf) and energy dissipation (ΔD) of an oscillating piezo-quartz crystal sensor (the surface of which can be coated with different materials) as a result of mass change on the sensor surface. Fe and Al oxide sensors (QSX326 and QSX309, respectively, Biolin Scientific) were used as the model mineral surfaces. The metal oxide layer is amorphous and with a thickness of ∼50 nm based on information from the vendor. The isoelectric point of the Al oxide sensor was previously determined to be 8.7[37] and that of the Fe oxide's is generally close to that of Al oxide.[26,27] Prior to the experiment, the sensors were cleaned by immersion in 5% H_2O_2 for 5 min, rinsing with deionized (DI) water, drying with pure N_2 gas, followed by exposure to UV/ozone for 10 min.

Polyphosphate solutions were prepared in 100 mM NaCl by dilution from the 1 mg mL^{-1} stock solution to a final concentration of 0.05 mg mL^{-1}, and the pH was adjusted to the desired value (4.0, 6.0, 8.0, and 10.0 ± 0.2) using 0.1 M HCl or 0.1 M NaOH. NaCl solution (100 mM) without polyphosphate was used as the background (BG) solution. The QCM-D experiments consisted of three consecutive steps: (1) baseline equilibrium with the background electrolyte; (2) introduction and continuous flow of polyphosphate solution; and (3) return to background electrolytes. The solutions were delivered at a constant flow rate of 100 μL min^{-1} through each module using a peristaltic pump. The resonance frequency (Δf) and energy dissipation (ΔD) values of the fundamental tone (n = 1) and all other overtones (n = 3, 5, 7, 9, 11, and 13) were all monitored.

The frequency signal was analyzed with the Sauerbrey equation to calculate adsorption mass (nanogram per cm^2; ng cm^2) because the Sauerbrey equation is applicable to adsorption layers that are relatively rigid and have small $\Delta D/\Delta f$ ratios (<2 × 10^{-8}/Hz). The Sauerbrey equation gives a linear relationship between Δf_n and mass change on the resonator[36]

$$\frac{\Delta f_n}{n} = \frac{m_f}{C} = \frac{\rho_f h_f}{C}$$

where m_f is the areal mass density of the adlayer (which is not necessarily equivalent to the dry mass of the adsorbed sorbate), and ρ_f and h_f are the wet density and thickness of the adlayer, respectively. C is the mass sensitivity constant, which depends solely on the fundamental resonance frequency and properties

https://dx.doi.org/10.1021/acs.jpcc.0c06127
J. Phys. Chem. C XXXX, XXX, XXX−XXX

of the quartz crystal.[36] Signals (Δf, ΔD, and mass) from the third and fifth overtone were averaged and used for plotting. The fundamental tone is the harmonic with the lowest resonance frequency, and the overtones resonate with a higher frequency. The extra results from multiple harmonics not only provide relevant qualitative QCM information but also allow viscoelastic analysis.

NMR Characterization. Solution ^{31}P NMR spectra of the concentrated polyphosphate stock solutions (1 mg mL^{-1}) were collected on a Bruker AMX 400 MHz spectrometer operated at 162 MHz at 297 K. Data acquisition parameters are 90° pulse width, 6.5k data points (TD) over an acquisition time of 0.51 s, and a relaxation delay of 15 s. The chemical shift was calibrated using 85% H_3PO_4 as the external standard. Solid-state ^{31}P NMR characterization was only conducted for 15P and 60P because of the overall similarity in 60P and 130P adsorption behaviors (detailed in the Results and Discussion section). Solid-state ^{31}P NMR spectroscopy was used to characterize polyphosphate adsorption on Al oxide only because the paramagnetic nature of Fe makes it highly challenging to conduct NMR measurements for the Fe oxide system.[38] Briefly, 200 mg of γ-Al_2O_3 was weighted into a 50 mL polystyrene centrifuge tube and combined with 20 mL of 0.05 mg mL^{-1} polyphosphate solution in 100 mM NaCl. The pH value of the suspension was adjusted to 6 or 10 at the beginning of the adsorption experiments and every 1.5 h afterward. Adsorption experiments were conducted for 3 and 24 h to evaluate the potential effects of adsorption time. At the end of the experiments, the solid product and supernatant were separated by centrifugation, and the solids were washed twice with DI water before freeze-drying. The obtained solid samples and initial polyphosphate sodium salts (15P, 60P, and 130P) were further characterized by solid-state ^{31}P NMR.

Direct polarization (DP) solid-state ^{31}P NMR spectra were acquired on pure polyphosphate sodium salts and polyphosphate-loaded minerals with magic angle spinning (MAS) and proton decoupling on a Bruker AVANCE 400 spectrometer operated at a ^{31}P frequency of 161.9 MHz. Samples (~20 mg) were packed into the insert, which was then fit into a 4 mm diameter zirconia rotor with Kel-F Caps (Wilmad, NJ) and spun at 12 kHz. Data collection parameters were 2048 data points (TD) over an acquisition time (AQ) of 12.6 ms and a recycle delay (RD) of 120 s. Variable RD experiments were conducted, and 120 s was sufficient to prevent signal saturation during data acquisition for the samples. The DP-MAS ^{31}P NMR spectra were acquired with a ^{31}P 90° pulse of 5.0 μs and an attenuation level (PL1) of 12.1 dB. Chemical shifts were externally referenced to $NH_4H_2PO_4$ at 0.72 ppm.

ATR−FTIR Characterization. The experimental IR setup and procedures were similar to previous studies.[16,28] ATR−FTIR spectra were recorded on a PerkinElmer Spectrum 100 spectrometer equipped with a Balston-Parker purge gas generator and a liquid N_2-cooled mercury-cadmium-telluride (MCT-A) detector. IR spectra of dissolved polyphosphate and of polyphosphate adsorbed onto Fe- and Al-oxides were collected using a horizontal ZnSe crystal (45° incidence angle, 10 internal reflections). Aqueous spectra were measured by scanning concentrated polyphosphate solutions (3P at 10 mM, 15P and 60P at 10 mg mL^{-1}) adjusted to pH 6.0 or 9.5. The spectra were the average of 200 scans collected in the 1450−750 cm^{-1} spectral range at a resolution of 4 cm^{-1}. Absorption bands in this wavenumber region originate primarily from the stretching vibrations of the phosphate groups in polyphosphate molecules.[29] A background spectrum of water was collected and subtracted from the polyphosphate solution spectra to isolate the polyphosphate vibrations.

ATR−FTIR spectra of 15P and 60P adsorbed on hematite (α-Fe_2O_3) and γ-alumina (γ-Al_2O_3) were collected and compared with that of adsorbed tripolyphosphate (3P; the shortest polyphosphate) to elucidate the polyphosphate complexation mechanisms. Additional experiments using 3P for IR study help assign IR peak positions of long-chained polyphosphate since IR spectra of 3P solution and 3P surface complexes on Fe/Al oxides were extensively studied.[13,30] These adsorption experiments were conducted with the flow-cell setup as previously described.[16,28] The ZnSe crystal was coated with a γ-Al_2O_3 or α-Fe_2O_3 film (2.5 mg) by drying 500 μL of a 5 g L^{-1} γ-Al_2O_3 or α-Fe_2O_3 suspension spread evenly across the surface, producing a stable and homogeneous deposit. A new deposit of γ-Al_2O_3 or α-Fe_2O_3 was prepared for each adsorption experiment. The coated crystal was sealed in a flow cell, which was installed on the ATR stage inside the FTIR spectrometer and connected to a reaction vessel containing 100 mL of 0.1 M NaCl electrolyte. The solution in the reaction vessel was magnetically stirred and set to the desired pH. The solution from the reaction vessel was passed through the flow cell at a rate of 0.5 mL min^{-1} using a peristaltic pump, and the effluent was circulated back into the vessel. Solution pH was monitored and readjusted with small aliquots of 0.1 M NaOH or 0.1 M HCl as necessary. The deposit of γ-Al_2O_3 or α-Fe_2O_3 was equilibrated with the background solution for 2.5 h. A final background spectrum consisting of the combined absorbances of the ZnSe crystal, the mineral deposit, and the background electrolyte was collected as the average of 200 scans at a resolution of 4 cm^{-1}. Next, the vessel was spiked with a concentrated polyphosphate stock solute to achieve concentrations of 125 μM (3P) or 50 mg L^{-1} (15P and 60P) in the reaction vessel. Polyphosphate adsorption on the mineral deposit was monitored by ratioing the IR spectra of the mineral film against the background spectrum collected at the end of pre-equilibration. After 2 h, the final spectrum of adsorbed polyphosphate was collected as the average of 200 scans at 4 cm^{-1} resolution in the spectral range 1450−750 cm^{-1}. The experiments were conducted at pH 6.0 and 9.5.

RESULTS AND DISCUSSION

Polyphosphate Characterization. Solution ^{31}P NMR spectrum of 15P stock solution displays a distinctive peak for polyphosphate end P groups at around −9.01 ppm, whereas the spectra of long-chained polyphosphates (60P and 130P) containing more middle P groups (chemical shift at −22 ppm) show the negligible intensity of end P group signal (Figure 1a), and the detailed descriptions were shown in our recent study.[20] The average chain length of a polyphosphate molecule can be calculated based on the ratio of the ^{31}P NMR peak area between the end P groups and total P groups.[20,39] The calculated ratios of end P to total P are ~0.15 (close to 2/15) for 15P, 0.033 (close to 2/60) for 60P, and 0.015 (close to 2/130) for 130P.

Solid-state NMR spectra of the three polyphosphate sodium salts (15P, 60P, and 130P) mainly contain the chemical signal of middle P groups at a chemical shift of ~−22 ppm, confirming that each polyphosphate has a narrow distribution of chain length without short-chained polyphosphate impurities (Figure 1b). The 15P salt contains a small amount of

https://dx.doi.org/10.1021/acs.jpcc.0c06127
J. Phys. Chem. C XXXX, XXX, XXX−XXX

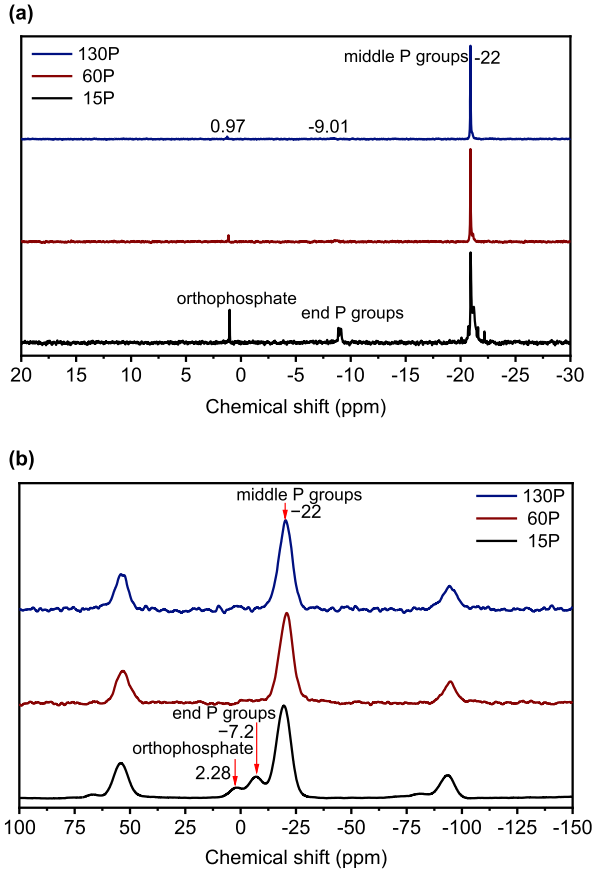

Figure 1. (a) Solution and (b) solid-state ^{31}P NMR spectra of 15P, 60P, and 130P polyphosphate stock solutions and sodium salts. Figure 1a data in our recent publication.[20]

orthophosphate impurity. Specifically, its solid-state NMR spectrum has two small peaks at ∼2.28 and ∼−7.2 ppm, possibly belonging to the chemical shifts of NaH_2PO_4 (2.6 ppm) and $NaH_2P_2O_7$ (−8.2 ppm), respectively.[40,41] The chemical shift at 0.97 ppm in 15P solution NMR spectrum is assigned to orthophosphate, and no separate peak for end P groups is observed (Figure 1a), suggesting the absence of pyrophosphate. Therefore, the chemical shifts at around 2.28 and −7.2 ppm in the 15P solid-state NMR spectrum are attributed to orthophosphate impurity and the end P groups of polyphosphates, respectively.

Polyphosphate Adsorption Measured by QCM-D: Signal Interpretation. QCM-D monitors temporal changes in frequency (Δf) and energy dissipation (ΔD), which is used to determine the adsorption kinetics and extent of polyphosphates onto metal oxide sensor surfaces (Figure 2). A decrease in frequency ($\Delta f < 0$) following the introduction of polyphosphate indicates the initiation of adsorption, and stabilization of the signal suggests adsorption saturation (Figures 2a,b and S1). The QCM-D profiles clearly show that polyphosphate adsorption (i.e., adsorption weight mass) experiences a rapid initial phase and reaches a steady state at ∼5 min (as Δf has no obvious change after 5 min), followed by a slow phase (Figure 2a,b). No obvious difference in adsorption behaviors of the three polyphosphates was observed. The fast adsorption and similarity among different polyphosphates suggest that the adsorption is not diffusion-limited because the sorbent is a flat surface and polyphosphates are relatively small molecules as compared to macromolecules such as proteins or organic matters.[36] After switching back to the background electrolyte, the frequency signal only shifted slightly (Δf becomes less negative), suggesting that the adsorption is overall irreversible and only a small fraction of adsorbed polyphosphates can be desorbed, implying the potential formation of inner-sphere surface complexes. Energy dissipation (ΔD) correlates with frequency signal, with ΔD value increasing with Δf. The frequency data is converted to adsorption mass using the Sauerbrey equation and correlation between ΔD and Δf is made to enable quantitative analysis of the effects of polyphosphate chain length and solution chemistry (Figures 2 and 3). The original QCM-D data are shown in Figures 2a,b and S1−3.

Polyphosphate Adsorption Measured by QCM-D: Effects of Chain Length and pH. Differences in compound molecular weight and adsorption configurations on mineral surfaces may lead to a difference in adsorption density and mass. Therefore, we compare the adsorption mass for the three polyphosphates onto Fe and Al oxide surfaces, the surface area of which is constant (Figure 2c,d). The adsorption amount of the three polyphosphates on both surfaces range from 90 to 120 ng/cm^2. Despite a big difference in molecular weight, no significant difference in adsorption amount is observed (Figure 2c). The data suggests similar surface adsorption density (numbers of P per cm^2) for the three polyphosphates, which is related to their adsorption configuration as discussed below. The surface charge of metal oxides is modulated by solution pH and commonly affects the adsorption of ionic species. Therefore, polyphosphate adsorption onto the two oxide surfaces is tested at pH ranging from 4 to 10. The results show maximal adsorption (∼120 ng/cm^2) at pH 6−8 and lowest adsorption (around 20−45 ng/cm^2) at pH 10 (Figure 2d). At the tested pH range, polyphosphates remain negatively charged (pK_{a1} of orthophosphate is ∼2.2), while metal oxides change from positively charged to negatively charged as pH shifts from acidic to alkaline, as both oxides have a point-of-zero charge of ∼9 (specifically 8.7 for this Al oxide sensor and 8.8 for hematite).[27] Thus, polyphosphate and oxide surfaces are oppositely charged and the adsorption is electrostatically favorable at pH below 9. However, polyphosphates become more protonated as pH decreases to 4, which compensates the effects of protonation on the mineral surface, resulting in less adsorption amount on Fe/Al oxides. Adsorption at pH 10 is significantly reduced (20−35% of the maximum) because the adsorption is under electrostatic repulsion. Such pH-dependent adsorption behavior suggests that polyphosphate adsorption is most likely driven by electrostatic interaction.

We also analyze the energy dissipation (ΔD) data by plotting the ΔD and Δf correlation to further probe the possible configuration of polyphosphates on oxide surfaces. Overall, the ΔD to Δf ratio ranges between −0.01 and −0.1 (10^{-6}/Hz), which is comparable to that of humic substances [around −0.1 to −0.7 (10^{-6}/Hz)][42−44] but much smaller than that of macromolecules [around −0.2 to −2.83 (10^{-6}/Hz)] such as DNA and proteins.[45,46] The small ratios suggest a relatively rigid and compact layer on the oxide surfaces. Polyphosphates are linear molecules of approximate 2.46, 9.39, and 20 nm in size (based on the reported length of P−O bond of 1.54 Å[47]) for 15P, 60P, and 130P, respectively. If they adsorb with one of the terminal groups and the rest of the molecule tailing into the solution, they may form a layer with different thicknesses and adsorbed mass (i.e., longer polyphosphate will form a thicker layer and have more adsorption

https://dx.doi.org/10.1021/acs.jpcc.0c06127
J. Phys. Chem. C XXXX, XXX, XXX−XXX

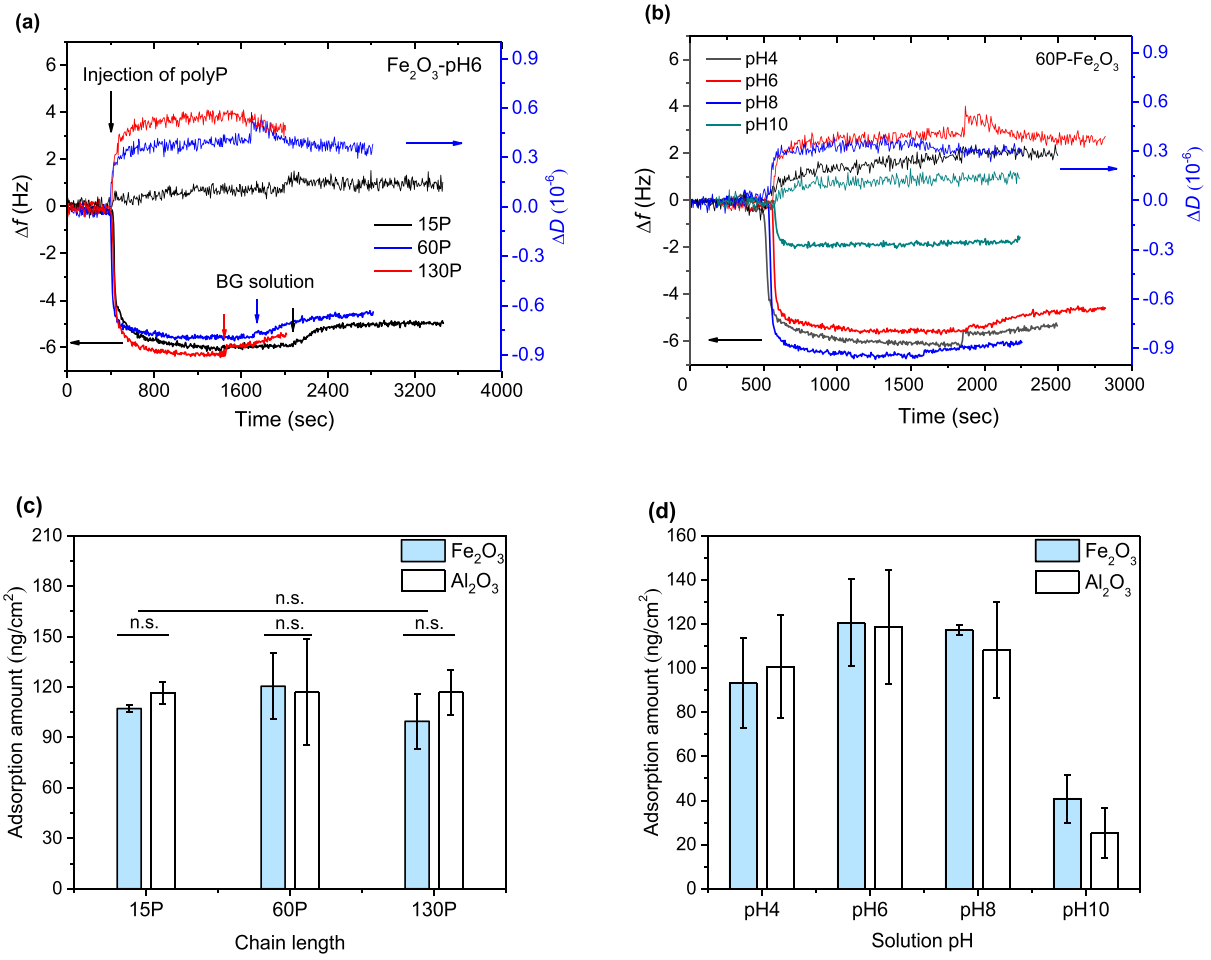

Figure 2. Selected QCM-D data (temporal frequency and energy dissipation shift) for the adsorption of three polyphosphates (15P, 60P, and 130P) at (a) pH6.0 and (b) for 60P adsorption at pH 4 to 10 on Fe oxide. The corresponding adsorption mass data on Fe and Al oxides were calculated by the Sauerbrey equation and presented in (c,d), respectively (n = 2 to 4). Significant difference was analyzed by Student's t-test and n.s. indicates no significant difference. Error bars represent standard deviation.

mass). Although 60P and 130P have a relatively larger ΔD to Δf ratio than that of 15P, all ratios are relatively small (humic substances with similar Δf and ΔD possess a thickness of <2 nm).[42,44] In addition, they have similar adsorption mass (i.e., similar numbers of P per cm^2). Because of the linear structure of the polyphosphate, it is very likely that the molecules "laid flat" on the sensor surface, instead of tailing into the bulk solution.

Spectroscopic Characterization of Polyphosphate–Mineral Interaction. Although bulk adsorption data by QCM-D suggest that the polyphosphate molecules laid flat on the oxide surface instead of tailing up, the chemical nature of the interaction is unknown. With monolayer adsorption configuration, surface adsorption density (numbers of P per cm^2) is similar among all three polyphosphates. We thus applied solid-state ^{31}P NMR and ATR–FTIR to determine surface coordination structure of polyphosphate on the oxides. Considering the molecular configuration of polyphosphates, several interaction modes might occur: (1) outer-sphere complexation between polyphosphate and minerals; (2) inner-sphere complexation (bidentate or monodentate) via one terminal P group and outer-sphere complexation via some of the middle P groups; and (3) inner-sphere complexation via both terminal P groups and some of the middle P groups (which can only be monodentate).

Solid-state ^{31}P NMR spectra of γ-Al_2O_3-bound polyphosphates (both 15P and 60P) show a major change as compared to the spectra of the corresponding free polyphosphate ions, specifically an enhancement of the chemical shift at ∼−11.1 ppm and the increase of its height with increasing reaction time (Figure 4). Although this chemical shift may have a contribution from the terminal P groups (−9.01 ppm; Figure 1a), the peak intensity is disproportionally large, considering the ratio of terminal P to total P in polyphosphate molecules. It is likely that this chemical shift is partially originated from the complexation of middle P groups with Al_2O_3 surface.[17] Middle P groups of free polyphosphates have a chemical shift at −22.1 ppm, and their complexation with Al_2O_3 through P−O−Al bonds may de-shield electrons of the P nuclei, resulting in the peak shifting toward higher chemical shift. Thus, the NMR chemical shift at −11.1 ppm can be assigned to inner-sphere complexes of polyphosphates (both terminal and middle P groups) on γ-Al_2O_3.[17] Li et al. (2013) summarized ^{31}P NMR chemical shift of different P compounds and different P sorption species and pointed out that the signals of inner-sphere P complexes typically appear between 0 and −11 ppm.[48] Enhancement of the chemical shift at −11.1 ppm in the 24 h reaction samples compared to 3 h samples further indicates an increase in the fraction of middle P complexed to the mineral surface. Although the attachment of polyphosphate

https://dx.doi.org/10.1021/acs.jpcc.0c06127
J. Phys. Chem. C XXXX, XXX, XXX−XXX

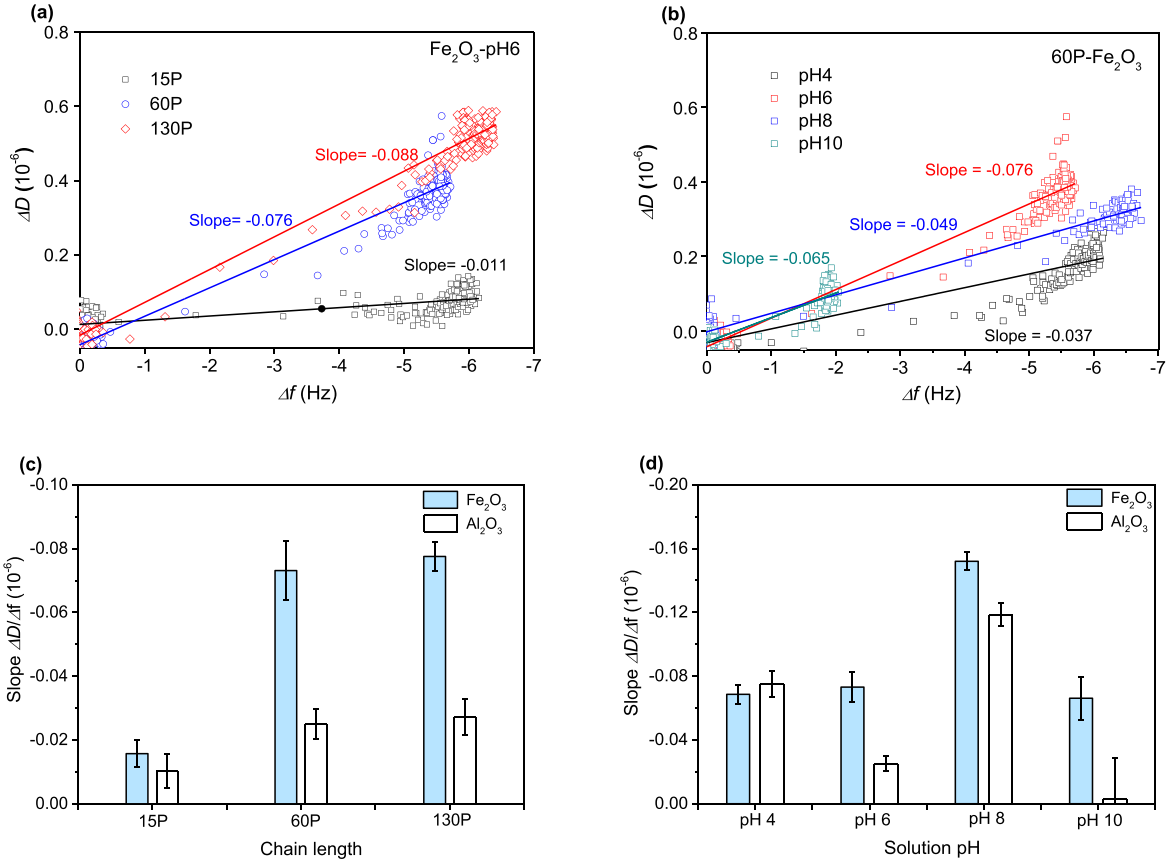

Figure 3. Selected energy dissipation and frequency correlation for adsorption of (a) three polyphosphates at pH 6.0 and (b) adsorption of 60P at pH 4 to 10 on Fe oxide. The data were linearly fitted, and the slope has been listed. Slopes from all replicates were averaged and plotted for adsorption of (c) three polyphosphate forms at pH 6.0 and (d) for the adsorption of 60P at different pHs on Fe and Al oxides. Error bars represent standard deviation (n = 2 − 4).

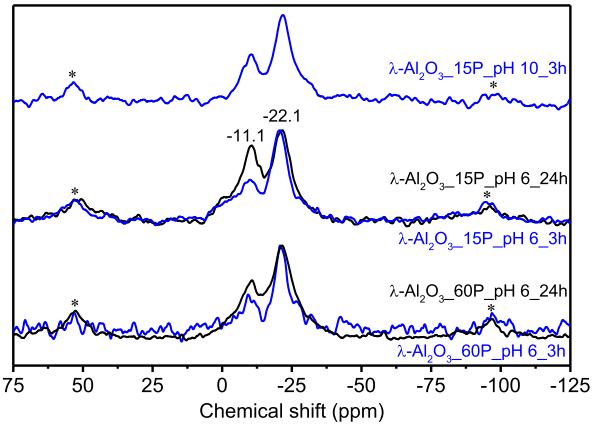

Figure 4. Solid-state ^{31}P NMR spectra of γ-Al_2O_3 bounded polyphosphates (15P and 60P) from 3 h and 24 h batch adsorption experiments at pH 6.0 and 10.0. Asterisks denote spinning side bands.

molecules to the mineral surface is relatively fast (as evidenced by QCM-D that adsorption steady state was reached within 5 min), the elastic linear molecules may experience gradual reconfiguration to maximize the bonding with mineral surface following the initial attachment of terminal P groups.

Interactions between polyphosphates and Fe/Al oxides were also characterized by *in situ* ATR−FTIR spectroscopy, assuming that vibration modes of polyphosphate molecules may change following surface interaction. ATR−FTIR spectra of 3P, 15P, and 60P in solution and adsorption on α-Fe_2O_3 and γ-Al_2O_3 at pH 6.0 and 9.5 were collected (Figure 5). IR spectra of free polyphosphate ions in the solutions show several characteristic peaks (Figure 5a and Table 1): (1) IR bands in the 1200−1300 cm^{-1} region are assigned to the asymmetric stretching vibrations of the bridging O−P−O [ν_{as}(O−P−O)], and the peak position moves to high wavenumber as polyphosphate chain length increases;[29,31] (2) IR band near 910 cm^{-1} (3P, 910 cm^{-1}; 15P, 917 cm^{-1}; and 60P, 917 cm^{-1}) belongs to the asymmetric stretching vibration of P−O−P [ν_{as}(P−O−P)];[29,31] and (3) IR bands appearing in the 930−1200 cm^{-1} region are attributed to the asymmetric or symmetric stretching vibrations of the P−O in different P units/structures (e.g., P−OH, PO_2^-, PO_3^{2-}, and $P_2O_7^{4-}$).[13,29,31] At pH 9.5, the newly appearing IR band for 15P (1359 cm^{-1}) and 60P (1363 cm^{-1}) originates from harmonics of ν_{as}(P═O) modes due to the high deprotonation of long-chain polyphosphate molecules under alkaline conditions.[49]

Following surface adsorption, IR bands of all three polyphosphates experienced either shifting or significant intensity changes, although differences between different oxide minerals and solution pH were relatively small (Figure 5b−d). The overall spectral similarity between polyphosphate adsorption to α-Fe_2O_3 at pH 6.0 and 9.5 suggests a similar interaction mode, which is consistent with the results of polyphosphate adsorption on TiO_2.[31] Therefore, we focus the

https://dx.doi.org/10.1021/acs.jpcc.0c06127
J. Phys. Chem. C XXXX, XXX, XXX−XXX

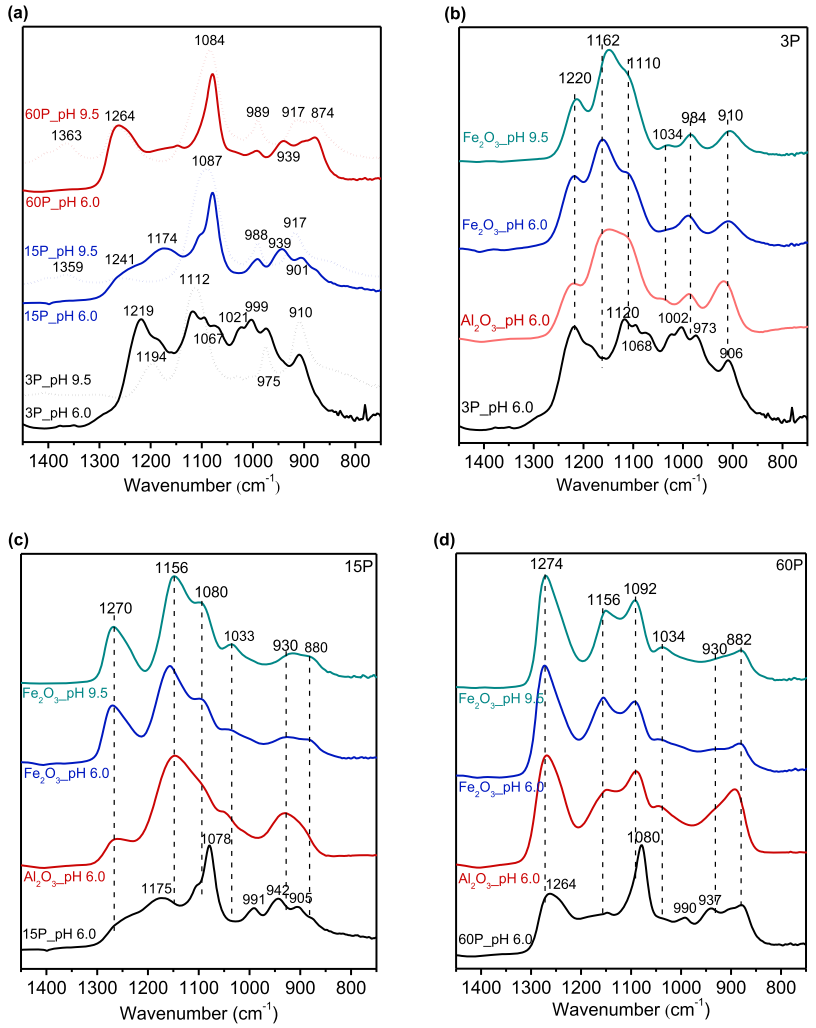

Figure 5. ATR−FTIR spectra of polyphosphates adsorbed on α-Fe_2O_3 and γ-Al_2O_3 at various pHs. (a) IR spectra of 3P, 15P, and 60P stock solutions at pH 6.0 and 9.5. ATR−FTIR spectra of (b) 3P, (c) 15P, and (d) 60P surface complexes on α-Fe_2O_3 and γ-Al_2O_3 at pH 6.0 and 9.5. All ATR−FTIR spectra were recorded in the 0.1 M NaCl background electrolytes and at a total polyphosphate concentration of 125 μM (3P) or 50 mg L^{-1} (15P and 60P).

discussion on adsorption at pH 6.0. Several spectral features after mineral adsorption are identified, and all three polyphosphates share two similar features: (1) the IR bands of surface-complexed polyphosphates in the regions of 1200−1300 and 1080−1110 cm^{-1} belong to the asymmetric and symmetric stretching vibrations of the bridging O−P−O [ν_{as}(O−P−O)] and O−P−O [ν_s(O−P−O)], respectively (Table 1); (2) the newly appeared bands near 1160 and 1033 cm^{-1} originate from the formation of inner-sphere phosphate complexes on α-Fe_2O_3 and γ-Al_2O_3 and belong to the asymmetric and symmetric stretching vibrations of surface Fe/Al atom-bonded phosphate groups [ν_{as}(P−O in ≡Fe/Al−PO_3) and ν_s(P−O in ≡Fe/Al−PO_3)], respectively.[13,29,31] Differences between short and long polyphosphates are also observed: (1) for the IR spectra of 3P adsorption on α-Fe_2O_3 and γ-Al_2O_3, the bands at 990 and 910 cm^{-1} are assigned to the asymmetric stretching vibrations of $P_2O_7^{3-}$ [ν_{as}($P_2O_7^{3-}$)] and P−O−P [ν_{as}(P−O−P)] because of the similar IR band positions in 3P solution (Figure 5b and Table 1). The presence of unbonded $P_2O_7^{3-}$ structure means that only one terminal phosphate group of 3P possibly complexes with surface Fe or Al atoms;[13] (2) for the IR spectra of 15P and 60P adsorption on α-Fe_2O_3 and γ-Al_2O_3, the IR bands at around 930 and 880 cm^{-1} are attributed to the asymmetric stretching vibrations of P−O−H [ν_{as}(P−O−H)] and P−O−P [ν_{as}(P−O−P)] in long-chain polyphosphates, respectively (Table 1). The presence of ν_{as}(P−O−H) implies that some middle P groups might not be associated with α-Fe_2O_3/γ-Al_2O_3 surface.

Regarding the effect of oxide surface, the numbers and positions of IR bands on α-Fe_2O_3 and γ-Al_2O_3 are similar, though with different intensities. The similar band number and position suggest that the surface P species and symmetry are similar on these two oxides. However, the intensity of the adsorption band at 1156 cm^{-1} is higher on α-Fe_2O_3 than on γ-Al_2O_3, possibly caused by the binding of more phosphate groups per polyphosphate molecule to Fe oxide than to Al oxide.[26,27]

Mechanisms of Polyphosphate−Mineral Interaction. For natural Fe and Al oxide minerals, their crystal facets are populated by singly, doubly, and triply coordinated hydroxyl groups, and surface hydroxyl (i.e., singly and triply coordinated surface hydroxyls) configuration is responsible for phosphate adsorption on these oxide minerals via surface ligand exchange.[50] However, these oxide minerals have different solubility product constants (K_{sp}), which may affect their adsorption capacity under different pH conditions. For

https://dx.doi.org/10.1021/acs.jpcc.0c06127
J. Phys. Chem. C XXXX, XXX, XXX−XXX

Table 1. Assignments of FTIR Peaks for Polyphosphate Solution (Left) and Polyphosphate Adsorption on α-Fe_2O_3 and γ-Al_2O_3 (Right)[13,29,31,49]

polyphosphate	wavenumber (cm^{-1})	assignments (free)	wavenumber (cm^{-1})	assignments (surface-bound)
3P	1219	ν_{as}(P−O in bridging O−P−O)		
	1194	ν_{as}(P−O in terminalHPO_3^-/H_2PO_3)	1220	ν_{as}(P−O in bridging PO_2^-)
	1112	ν_{as}(P−O in terminal PO_3^{2-})	1162	ν_{as}(P−O in ≡Fe/Al−PO_3)
	1067	ν_{as}(P−O) in single P unit	1110	ν_s(P−O in bridging PO_2^-)
	1021	ν_{as}(P−OH in $HP_3O_{10}^{4-}$)	1034	ν_s(P−O in ≡Fe/Al−PO_3)
	999	ν_s(P−OH in $HP_3O_{10}^{4-}$)	990	$\nu_{as}(P_2O_7^{4-})$
	975	$\nu_{as}(P_2O_7^{4-})$	910	ν_{as}(P−O−P)
	910	ν_{as}(P−O−P)		
15P	1359	harmonics of ν_{as}(P═O) modes		
	1241	ν_{as}(P−O in bridging O−P−O)	1270	ν_{as}(P−O in bridging PO_2^-)
	1174	ν_{as}(P−O in terminal HPO_3^-/H_2PO_3)	1156	ν_{as}(P−O in ≡Fe/Al−PO_3)
	1087	ν_{as}(P−O) in single P unit	1080	ν_s(P−O in bridging PO_2^-)
	988	$\nu_{as}(P_2O_7^{4-})$	1033	ν_s(P−O in ≡Fe/Al−PO_3)
	939	ν_{as}(P−OH)	930	ν_{as}(P−O−H)
	917	ν_{as}(P−O−P)	876	ν_{as}(P−O−P)
60P	1363	harmonics of ν_{as}(P═O) modes		
	1264	ν_{as}(P−O in bridging PO_2^-)	1274	ν_{as}(P−O in bridging PO_2^-)
	1084	ν_{as}(P−O) in single P unit	1156	ν_{as}(P−O in ≡Fe/Al−PO_3)
	989	$\nu_{as}(P_2O_7^{4-})$	1092	ν_s(P−O in bridging PO_2^-)
	939	ν_{as}(P−OH)	1034	ν_s(P−O in ═Fe/Al−PO_3)
	917	ν_{as}(P−O−P)	930	ν_{as}(P−O−H)
	871	ν_s(P−O−P)	882	ν_{as}(P−O−P)

example, Al oxides have a higher solubility at acidic pH than Fe oxides and can also dissolve rapidly at alkaline pH to release $Al(OH)_4^-$, which decreases the solid mass of Al oxides for phosphate adsorption under highly alkaline conditions.[51,52] This might be reflected in the low adsorption amount of polyphosphate on the Al oxide sensor at pH 10 (Figure 2d).

Previous studies show that orthophosphate and *myo*-inositol hexakisphosphate adsorption on Fe and Al (oxyhydr)oxides generally occurs through the formation of bidentate binuclear surface complexes via surface ligand exchange.[17,22,38,53] Polyphosphates differ from these molecules in that they have a chain of middle P groups that can also interact with mineral surfaces in addition to the terminal phosphate groups and in that polyphosphates with different chain lengths possess different molecular elasticities. Our recent research revealed that polyphosphates can be readily hydrolyzed on Al and manganese (Mn) oxide surfaces via the gradual cleavage of the terminal P groups, suggesting the tendency of polyphosphate terminal P groups to form bidentate binuclear complexes with surface Mn/Al atoms.[17,20,54] According to QCM results, the adsorption amount (surface density of P unit) is similar for polyphosphates with different chain lengths. This suggests that polyphosphate molecules may adopt a lay-down configuration on mineral surfaces. Solid-state ^{31}P NMR and ATR−FTIR results substantiate the involvement of a fraction of middle P groups in surface interaction through the formation of monodentate mononuclear surface complexes. Therefore, although terminal P groups may possess a stronger affinity than middle P groups for the mineral surface, the elastic linear structure of polyphosphate molecules enables them to bend and have more contact with mineral surfaces. Because of the structural constraint and spatial mismatch, it is unlikely that all middle P moieties complex with surface Fe or Al atoms; this is evidenced in the FTIR observation of 3P adsorption that the interaction involves only a terminal P group and of ν_{as}(P−O−H) presence in polyphosphate surface complexes on Fe/Al oxides. Based on these findings, we propose that the potential scheme of polyphosphate interaction on the surface of Fe/Al oxides is via the formation of bidentate binuclear surface complexes for terminal P groups and monodentate mononuclear surface complexes for a fraction of middle P groups (Figure 6).

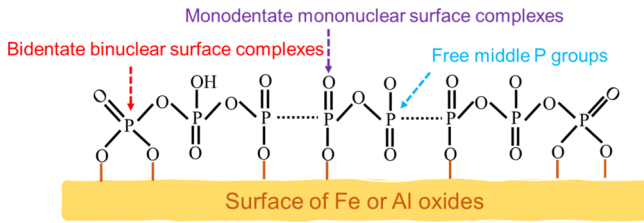

Figure 6. Schematic illustration for the potential coordination structures of polyphosphate adsorption on Fe or Al oxide, based on QCM-D and spectroscopic analyses. Two terminal P groups may form bidentate binuclear surface complexes, and a fraction of middle P groups may form monodentate mononuclear surface complexes on Fe or Al oxides.

■ CONCLUSIONS AND PERSPECTIVES

The findings from this study suggest that polyphosphates adsorb on Fe/Al oxides via the formation of inner-sphere surface complexes under environmental pH conditions and Fe/Al oxide-immobilized polyphosphates may resist strong desorption. Our results provide new insights into polyphosphate interfacial chemistry as we provide the first combined QCM-D and spectroscopy evidence on the possible coordination symmetry of polyphosphate on oxide minerals. QCM-D determines that the polyphosphate molecules lay down on the mineral surface, and IR and NMR spectroscopies provide the molecular binding information and time-resolved dynamics of phosphate surface complexation. The methodology may be

https://dx.doi.org/10.1021/acs.jpcc.0c06127
J. Phys. Chem. C XXXX, XXX, XXX−XXX

applied to investigate the molecular mechanism on the interfacial reactions of other phosphate species or polymers (e.g., extracellular polymeric substances and natural organic matters) at the mineral−water interface. Further studies are warranted to assess the impacts of other environmental factors (such as chelating cations, competitive anions, and dissolved organic matter) to better understand the interfacial behaviors governing the fate, transport, and bioavailability of polyphosphate or other P species in complex environmental settings.

■ ASSOCIATED CONTENT

Supporting Information

The Supporting Information is available free of charge at https://pubs.acs.org/doi/10.1021/acs.jpcc.0c06127.

Data on QCM-D frequency and dissipation change due to polyphosphate adsorption on Fe or Al oxide surface (PDF)

■ AUTHOR INFORMATION

Corresponding Authors

Rixiang Huang − *Department of Environmental and Sustainable Engineering, University at Albany, State University of New York, Albany, New York 12222, United States*; Phone: 518-437-4977; Email: rhuang6@albany.edu

Yuanzhi Tang − *School of Earth and Atmospheric Sciences, Georgia Institute of Technology, Atlanta, Georgia 30332-0340, United States*; orcid.org/0000-0002-7741-8646; Phone: 404-894-3814; Email: yuanzhi.tang@eas.gatech.edu

Authors

Biao Wan − *School of Earth and Atmospheric Sciences, Georgia Institute of Technology, Atlanta, Georgia 30332-0340, United States*

Evert J. Elzinga − *Department of Earth & Environmental Sciences, Rutgers University, Newark, New Jersey 07102, United States*; orcid.org/0000-0003-4781-7272

Complete contact information is available at: https://pubs.acs.org/10.1021/acs.jpcc.0c06127

Notes

The authors declare no competing financial interest.

■ ACKNOWLEDGMENTS

This work was supported by the US National Science Foundation (NSF) under grants# 1559087, 1739884, and 1559124. B.W. acknowledges support from the China Scholarship Council (CSC) under grants #201606760059.

■ REFERENCES

(1) Paytan, A.; McLaughlin, K. The oceanic phosphorus cycle. *Chem. Rev.* **2007**, *107*, 563−576.

(2) Van Mooy, B. A. S.; Krupke, A.; Dyhrman, S. T.; Fredricks, H. F.; Frischkorn, K. R.; Ossolinski, J. E.; Repeta, D. J.; Rouco, M.; Seewald, J. D.; Sylva, S. P. Major role of planktonic phosphate reduction in the marine phosphorus redox cycle. *Science* **2015**, *348*, 783−785.

(3) Omelon, S. J.; Grynpas, M. D. Relationships between polyphosphate chemistry, biochemistry and apatite biomineralization. *Chem. Rev.* **2008**, *108*, 4694−4715.

(4) Kulakovskaya, T. V.; Vagabov, V. M.; Kulaev, I. S. Inorganic polyphosphate in industry, agriculture and medicine: Modern state and outlook. *Process Biochem.* **2012**, *47*, 1−10.

(5) Zhang, F.; Blasiak, L. C.; Karolin, J. O.; Powell, R. J.; Geddes, C. D.; Hill, R. T. Phosphorus sequestration in the form of polyphosphate by microbial symbionts in marine sponges. *Proc. Natl. Acad. Sci. U.S.A.* **2015**, *112*, 4381−4386.

(6) Martin, P.; Dyhrman, S. T.; Lomas, M. W.; Poulton, N. J.; Van Mooy, B. A. S. Accumulation and enhanced cycling of polyphosphate by Sargasso Sea plankton in response to low phosphorus. *Proc. Natl. Acad. Sci. U.S.A.* **2014**, *111*, 8089−8094.

(7) Orchard, E. D.; Benitez-Nelson, C. R.; Pellechia, P. J.; Lomas, M. W.; Dyhrman, S. T. Polyphosphate in Trichodesmium from the low-phosphorus Sargasso Sea. *Limnol. Oceanogr.* **2010**, *55*, 2161−2169.

(8) Diaz, J.; Ingall, E.; Benitez-Nelson, C.; Paterson, D.; de Jonge, M. D.; McNulty, I.; Brandes, J. A. Marine polyphosphate: A key player in geologic phosphorus sequestration. *Science* **2008**, *320*, 652−655.

(9) Diaz, J. M.; Ingall, E. D.; Snow, S. D.; Benitez-Nelson, C. R.; Taillefert, M.; Brandes, J. A. Potential role of inorganic polyphosphate in the cycling of phosphorus within the hypoxic water column of Effingham Inlet, British Columbia. *Global Biogeochem. Cycles* **2012**, *26*, GB2040.

(10) Hupfer, M.; Ruübe, B.; Schmieder, P. Origin and diagenesis of polyphosphate in lake sediments: A ^{31}P-NMR study. *Limnol. Oceanogr.* **2004**, *49*, 1−10.

(11) Rashchi, F.; Finch, J. A. Polyphosphates: A review their chemistry and application with particular reference to mineral processing. *Miner. Eng.* **2000**, *13*, 1019−1035.

(12) Majed, N.; Matthäus, C.; Diem, M.; Gu, A. Z. Evaluation of intracellular polyphosphate dynamics in enhanced biological phosphorus eemoval process using Raman microscopy. *Environ. Sci. Technol.* **2009**, *43*, 5436−5442.

(13) Guan, X.-H.; Liu, Q.; Chen, G.-H.; Shang, C. Surface complexation of condensed phosphate to aluminum hydroxide: An ATR-FTIR spectroscopic investigation. *J. Colloid Interface Sci.* **2005**, *289*, 319−327.

(14) Sharpley, A. N.; Chapra, S. C.; Wedepohl, R.; Sims, J. T.; Daniel, T. C.; Reddy, K. R. Managing agricultural phosphorus for protection of aurface waters: Issues and options. *J. Environ. Qual.* **1994**, *23*, 437−451.

(15) Wan, B.; Yan, Y.; Liu, F.; Tan, W.; Chen, X.; Feng, X. Surface adsorption and precipitation of inositol hexakisphosphate on calcite: A comparison with orthophosphate. *Chem. Geol.* **2016**, *421*, 103−111.

(16) Wan, B.; Yan, Y. P.; Zhu, M. Q.; Wang, X. M.; Liu, F.; Tan, W. F.; Feng, X. H. Quantitative and spectroscopic investigations of the co-sorption of myo-inositol hexakisphosphate and cadmium(II) on to haematite. *Eurasian J. Soil Sci.* **2017**, *68*, 374−383.

(17) Wan, B.; Huang, R.; Diaz, J. M.; Tang, Y. Polyphosphate adsorption and hydrolysis on aluminum oxides. *Environ. Sci. Technol.* **2019**, *53*, 9542−9552.

(18) Liu, J.; Hu, Y.; Yang, J.; Abdi, D.; Cade-Menun, B. J. Investigation of soil legacy phosphorus transformation in long-term agricultural fields using sequential fractionation, P K-edge XANES and solution P NMR spectroscopy. *Environ. Sci. Technol.* **2015**, *49*, 168−176.

(19) Wood, T.; Bormann, F. H.; Voigt, G. K. Phosphorus cycling in a northern hardwood forest: Biological and chemical control. *Science* **1984**, *223*, 391−393.

(20) Huang, R.; Wan, B.; Hultz, M.; Diaz, J. M.; Tang, Y. Phosphatase-mediated hydrolysis of linear polyphosphates. *Environ. Sci. Technol.* **2018**, *52*, 1183−1190.

(21) Zhu, Y.; Wu, F.; Feng, W.; Liu, S.; Giesy, J. P. Interaction of alkaline phosphatase with minerals and sediments: Activities, kinetics and hydrolysis of organic phosphorus. *Colloids Surf., A* **2016**, *495*, 46−53.

(22) Yan, Y.; Koopal, L. K.; Li, W.; Zheng, A.; Yang, J.; Liu, F.; Feng, X. Size-dependent sorption of myo-inositol hexakisphosphate and orthophosphate on nano-γ-Al_2O_3. *J. Colloid Interface Sci.* **2015**, *451*, 85−92.

https://dx.doi.org/10.1021/acs.jpcc.0c06127
J. Phys. Chem. C XXXX, XXX, XXX−XXX

(23) Li, W.; Harrington, R.; Tang, Y.; Kubicki, J. D.; Aryanpour, M.; Reeder, R. J.; Parise, J. B.; Phillips, B. L. Differential pair distribution function study of the structure of arsenate adsorbed on nanocrystalline γ-alumina. *Environ. Sci. Technol.* **2011**, *45*, 9687−9692.
(24) Li, W.; Livi, K. J. T.; Xu, W.; Siebecker, M. G.; Wang, Y.; Phillips, B. L.; Sparks, D. L. Formation of crystalline Zn−Al layered double hydroxide precipitates on γ-alumina: The role of mineral dissolution. *Environ. Sci. Technol.* **2012**, *46*, 11670−11677.
(25) Ruttenberg, K. C.; Sulak, D. J. Sorption and desorption of dissolved organic phosphorus onto iron (oxyhydr)oxides in seawater. *Geochim. Cosmochim. Acta* **2011**, *75*, 4095−4112.
(26) Yan, Y. P.; Liu, F.; Li, W.; Liu, F.; Feng, X. H.; Sparks, D. L. Sorption and desorption characteristics of organic phosphates of different structures on aluminium (oxyhydr)oxides. *Eurasian J. Soil Sci.* **2014**, *65*, 308−317.
(27) Wang, X.; Liu, F.; Tan, W.; Li, W.; Feng, X.; Sparks, D. L. Characteristics of phosphate adsorption-desorption onto ferrihydrite: Comparison with well-crystalline Fe (hydr)oxides. *Soil Sci.* **2013**, *178*, 1−11.
(28) Barreto, M. S. C.; Elzinga, E. J.; Alleoni, L. R. F. Attenuated total reflectance−Fourier transform infrared study of the effects of citrate on the adsorption of phosphate at the hematite surface. *Soil Sci. Soc. Am. J.* **2020**, *84*, 57−67.
(29) Wan, B.; Yan, Y.; Tang, Y.; Bai, Y.; Liu, F.; Tan, W.; Huang, Q.; Feng, X. Effects of polyphosphates and orthophosphate on the dissolution and transformation of ZnO nanoparticles. *Chemosphere* **2017**, *176*, 255−265.
(30) Hamilton, J. G.; Hilger, D.; Peak, D. Mechanisms of tripolyphosphate adsorption and hydrolysis on goethite. *J. Colloid Interface Sci.* **2017**, *491*, 190−198.
(31) Michelmore, A.; Gong, W.; Jenkins, P.; Ralston, J. The interaction of linear polyphosphates with titanium dioxide surfaces. *Phys. Chem. Chem. Phys.* **2000**, *2*, 2985−2992.
(32) Li, W.; Wang, Y.-J.; Zhu, M.; Fan, T.-T.; Zhou, D.-M.; Phillips, B. L.; Sparks, D. L. Inhibition mechanisms of Zn precipitation on aluminum oxide by glyphosate: A ^{31}P NMR and Zn EXAFS study. *Environ. Sci. Technol.* **2013**, *47*, 4211−4219.
(33) Elzinga, E. J.; Sparks, D. L. Phosphate adsorption onto hematite: An in situ ATR-FTIR investigation of the effects of pH and loading level on the mode of phosphate surface complexation. *J. Colloid Interface Sci.* **2007**, *308*, 53−70.
(34) Nguyen, M. L.; Hockaday, W. C.; Lau, B. L. T. Is the adsorption of soil organic matter to haematite (α-Fe_2O_3) temperature dependent? *Eurasian J. Soil Sci.* **2018**, *69*, 892−901.
(35) Dixon, M. C. Quartz crystal microbalance with dissipation monitoring: Enabling real-time characterization of biological materials and their interactions. *J. Biomol. Tech.* **2008**, *19*, 151−158.
(36) Huang, R.; Yi, P.; Tang, Y. Probing the interactions of organic molecules, nanomaterials, and microbes with solid surfaces using quartz crystal microbalances: Methodology, advantages, and limitations. *Environ. Sci.: Processes Impacts* **2017**, *19*, 793−811.
(37) Cuddy, M. F.; Poda, A. R.; Brantley, L. N. Determination of isoelectric points and the role of pH for common quartz crystal microbalance sensors. *ACS Appl. Mater. Interfaces* **2013**, *5*, 3514−3518.
(38) Kim, J.; Li, W.; Philips, B. L.; Grey, C. P. Phosphate adsorption on the iron oxyhydroxides goethite (α-FeOOH), akaganeite (β-FeOOH), and lepidocrocite (γ-FeOOH): A ^{31}P NMR Study. *Energy Environ. Sci.* **2011**, *4*, 4298−4305.
(39) Fang, W.; Sheng, G.-P.; Wang, L.-F.; Ye, X.-D.; Yu, H.-Q. Quantitative evaluation of noncovalent interactions between polyphosphate and dissolved humic acids in aqueous conditions. *Environ. Pollut.* **2015**, *207*, 123−129.
(40) He, Z.; Honeycutt, C. W.; Xing, B.; McDowell, R. W.; Pellechia, P. J.; Zhang, T. Solid-stare Fourier transformation infrared and ^{31}P nuclear magnetic resonance spectral features of phosphate compounds. *Soil Sci.* **2007**, *172*, 501−515.
(41) Griffiths, L.; Root, A.; Harris, R. K.; Packer, K. J.; Chippendale, A. M.; Tromans, F. R. Magic-angle spinning phosphorus-31 nuclear magnetic resonance of polycrystalline sodium phosphates. *J. Chem. Soc., Dalton Trans.* **1986**, *10*, 2247−2251.
(42) Armanious, A.; Aeppli, M.; Sander, M. Dissolved organic matter adsorption to model surfaces: Adlayer formation, properties, and dynamics at the nanoscale. *Environ. Sci. Technol.* **2014**, *48*, 9420−9429.
(43) Li, W.; Liao, P.; Oldham, T.; Jiang, Y.; Pan, C.; Yuan, S.; Fortner, J. D. Real-time evaluation of natural organic matter deposition processes onto model environmental surfaces. *Water Res.* **2018**, *129*, 231−239.
(44) Yan, M.; Liu, C.; Wang, D.; Ni, J.; Cheng, J. Characterization of adsorption of humic acid onto alumina using quartz crystal microbalance with dissipation. *Langmuir* **2011**, *27*, 9860−9865.
(45) Nguyen, T. H.; Elimelech, M. Adsorption of Plasmid DNA to a Natural Organic Matter-Coated Silica Surface: Kinetics, Conformation, and Reversibility. *Langmuir* **2007**, *23*, 3273−3279.
(46) Jacobson, K. H.; Kuech, T. R.; Pedersen, J. A. Attachment of pathogenic prion protein to model oxide surfaces. *Environ. Sci. Technol.* **2013**, *47*, 6925−6934.
(47) Wang, Q.; Liao, X.; Xu, W.; Ren, Y.; Livi, K. J.; Zhu, M. Synthesis of birnessite in the presence of phosphate, silicate, or sulfate. *Inorg. Chem.* **2016**, *55*, 10248−10258.
(48) Li, W.; Pierre-Louis, A.-M.; Kwon, K. D.; Kubicki, J. D.; Strongin, D. R.; Phillips, B. L. Molecular level investigations of phosphate sorption on corundum (α-Al_2O_3) by ^{31}P solid state NMR, ATR-FTIR and quantum chemical calculation. *Geochim. Cosmochim. Acta* **2013**, *107*, 252−266.
(49) Jha, P. K.; Pandey, O. P.; Singh, K. FTIR spectral analysis and mechanical properties of sodium phosphate glass−ceramics. *J. Mol. Struct.* **2015**, *1083*, 278−285.
(50) Huang, X.; Foster, G. D.; Honeychuck, R. V.; Schreifels, J. A. The maximum of phosphate adsorption at pH 4.0: Why it appears on aluminum oxides but not on iron oxides. *Langmuir* **2009**, *25*, 4450−4461.
(51) Wan, B.; Yan, Y.; Huang, R.; Abdala, D. B.; Liu, F.; Tang, Y.; Tan, W.; Feng, X. Formation of Zn-Al layered double hydroxides (LDH) during the interaction of ZnO nanoparticles (NPs) with γ-Al_2O_3. *Sci. Total Environ.* **2019**, *650*, 1980−1987.
(52) Yan, Y.; Li, W.; Yang, J.; Zheng, A.; Liu, F.; Feng, X.; Sparks, D. L. Mechanism of myo-inositol hexakisphosphate sorption on amorphous aluminum hydroxide: Spectroscopic evidence for rapid surface precipitation. *Environ. Sci. Technol.* **2014**, *48*, 6735−6742.
(53) Yan, Y.; Wan, B.; Liu, F.; Tan, W.; Liu, M.; Feng, X. Adsorption-desorption of myo-inositol hexakisphosphate on hematite. *Soil Sci.* **2014**, *179*, 476−485.
(54) Wan, B.; Huang, R.; Diaz, J. M.; Tang, Y. Manganese oxide catalyzed hydrolysis of polyphosphates. *ACS Earth Space Chem.* **2019**, *3*, 2623−2634.

https://dx.doi.org/10.1021/acs.jpcc.0c06127
J. Phys. Chem. C XXXX, XXX, XXX−XXX